Synthesis, crystal structure, vibrational and ^{31}P-NMR spectroscopy of the thiophosphate NaMg[PO$_3$S]·9H$_2$O

Henning A. Höppe [a, *], Stefan W. Scharinger [a], Joachim G. Heck [b], Peter Gross [a], Philip Netzsch [a], Karolina Kazmierczak [a]

[a] Institut für Physik, Universität Augsburg, Universitätsstraße 1, D-86159, Augsburg, Germany
[b] Institute of Inorganic Chemistry, Karlsruhe Institute of Technology, Engesserstraße 15, D-76131, Karlsruhe, Germany

1. Introduction

Alkaline earth phosphates and respective homologues attract interest as possible host structures for doping with divalent rare earth ions such as Eu^{2+} to synthesise luminescent materials [1]. The absorption and emission of divalent europium are very efficient due to the participation of parity allowed $4f$–$5d$ transitions. The energies of these transitions are subject to crystal field splitting and nephelauxetic effects and thus depend strongly from the coordination environment.

All monothiophosphates derive from P$_4$O$_6$S$_4$ comprising solely [PO$_3$S] tetrahedra [2,3]. So far thiophosphates are known of the alkaline metals, such as Na$_3$[PO$_3$S]·12H$_2$O [4], Na$_3$[PO$_3$S] [5,6], KH$_2$[PO$_3$S] [7], and also of the monovalent cations biuret [8], and guanidinium [9]. Crystal structures of thiophosphates comprising trivalent ions are not yet known, but two of tetravalent ions, i. e. MH$_2$[PO$_3$S]$_2$ (M = Zr, Hf) [10]. Besides the basic interest concerning phosphors thiophosphates have also been interesting as possible ion conductors [5] or SHG active material [11].

In this context we started a systematic evaluation of partially substituted alkaline-earth phosphates like monothiophosphates comprising [PO$_3$S]$^{3-}$ tetrahedra. Recently, we reported about the crystal structures of NaCa[PO$_3$S]·9H$_2$O and NaBa[PO$_3$S]·9H$_2$O [12], which are isotypic with the respective strontium compound [13]. In this contribution we will shed light on the crystal structures of NaMg[PO$_3$S]·9H$_2$O at room temperature and − due to strongly vibrating anions at room temperature − at 100 K. Moreover, we present NMR and vibrational spectra to further confirm our structure model.

2. Results and discussion

2.1. Crystal structure at room temperature

NaMg[PO$_3$S]·9H$_2$O crystallises in the orthorhombic space group $Cmc2_1$ (no. 36) in its own structure type. In sodium magnesium thiophosphate nonahydrate slightly distorted Mg(OH$_2$)$_6$ octahedra share two edges with two neighbouring trigonal Na(OH$_2$)$_6$ prisms forming condensed chains running parallel [100] (Fig. 1), described by $\frac{1}{\infty}\left[\text{Na(H}_2\text{O)}_{\frac{4}{2}}\text{(H}_2\text{O)}_2\text{Mg(H}_2\text{O)}_{\frac{4}{2}}\text{(H}_2\text{O)}_2\right]^{3+}$. Terminal atoms of the thiophosphate tetrahedron shown in Fig. 2 contribute in neither

* Corresponding author.
 E-mail address: henning@ak-hoeppe.de (H.A. Höppe).
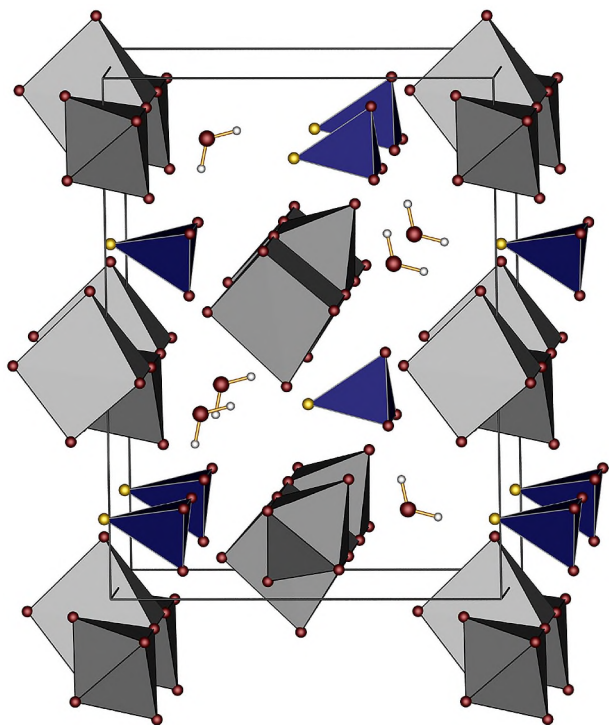
Fig. 1. Unit cell of NaMg[PO₃S]·9H₂O at room temperature viewed approx. along [100] — the PO₃S tetrahedra are drawn as closed polyhedra (sulphur atoms yellow, oxygen atoms red, sodium centred trigonal prisms medium grey, magnesium centred octahedra dark grey. (For interpretation of the references to colour in this figure legend, the reader is referred to the web version of this article.)
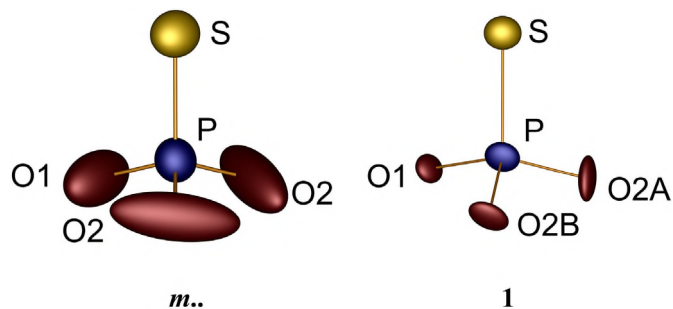
Fig. 2. PO₃S tetrahedron in NaMg[PO₃S]·9H₂O at room temperature (left) and at 100 K (right), ellipsoids drawn on a 90% probability level, the site symmetries of P are given (sulphur atoms yellow, oxygen atoms red and phosphorus blue). (For interpretation of the references to colour in this figure legend, the reader is referred to the web version of this article.)

case to the coordination sphere of sodium and magnesium, but are embedded into a hydrogen bond network to the crystal water molecules coordinating the metal ions. The P—S bonds point parallel [00$\bar{1}$] yielding a polar crystal structure (Fig. 1). At room temperature the anharmonic displacement parameters of the oxygen atoms O1 and O2 of the [PO₃S] tetrahedra are very large which points towards a rotational disorder around the P—S axis. This disorder cannot be resolved at room temperature using split positions of O1 and O2. The phosphorus atoms centre distorted tetrahedra of one sulphur and three oxygen atoms with bond lengths P—S of 204.7(1) pm and the P—O bonds ranging between 150.1(3) and 151.1(3) pm, both well close to the sum of ionic radii of 201 pm for P—S and 155 pm for P—O interactions [14]. Oxygen and sulphur are unequivocally ordered on their respective crystallographic sites.

Both, Na⁺ and Mg²⁺, are coordinated by six crystal water molecules with coordination distances Na-O$_W$ in the ranges 231.0(4) − 269.7(3) pm and 202.2(3) − 208.9(2) pm for Mg-O$_W$ (see Fig. 3). These ranges also coincide with the sum of ionic radii [14] of 240 pm and 210 pm, respectively. An overview about relevant bond-lengths and bonding angles delivers Table 3. Out of the seven crystallographically different water molecules only the one centred by OW4 does not coordinate at all to the cations, but is part of the extended hydrogen bond network. The angles O—H···O of the hydrogen bonds vary between 131 and 179°, thus according to *Steiner* [15] the bonds are classified between medium and strong. Table 1 gives an overview about the hydrogen bonds found in NaMg[PO₃S]·9H₂O.

2.2. Extended hydrogen bond network

The following description is based on the room temperature structure model, that of the low temperature form is analogous. Per formula unit a total of nine crystal water molecules is present in the crystal structure of NaMg[PO₃S]·9H₂O. These molecules spread over seven crystallographically independent sites (OW1…OW7) and form an extended structure assuming hydrogen-bonding interactions considering crystal water molecule donor acceptor distances below 310 pm (Table 1).

The crystal water sites OW3, OW4 (2×), OW5 and OW7 (2×) form almost regular octahedra hosting the smaller magnesium cations. Along [100] these are connected via OW1 bridges — branched to OW2 — to form infinite chains of bridged octahedra. Two edges of adjacent octahedra form two edges of a slightly distorted trigonal prism, the third edge of which is formed by OW5 and OW6 crystal water molecules. These prisms host the larger sodium cations.

In the crystal structure these chains of bridged octahedra form a hexagonal rod packing (Fig. 1). The PO₃S tetrahedra are relatively loosely coordinated in large cavities in-between consisting of fifteen crystal water molecules (1×OW1, 2×OW2, 2×OW3, 4×OW4, 2×OW5, 2×OW6, 2×OW7). These cavities comprise 37 distorted triangular faces and one distorted pentagonal face around the sulphur atom forming a rotunda.

2.3. Crystal structure at 100 K

As mentioned and shown (Fig. 2) before, the PO₃ S tetrahedron shows strong vibrations at room temperature around the P—S bond. To analyse this behaviour further we investigated the crystal structure at 100 K. Upon cooling the unit cell shrinks anisotropically. While *a* and *b* decrease as expected, the *c* parameter increases slightly (Table 2). Moreover, we observed a reduced symmetry of the crystal structure. Formally, the mirror and the glide planes of *Cmc*2₁ vanish giving the non-conventional space group *C*112₁, i. e.
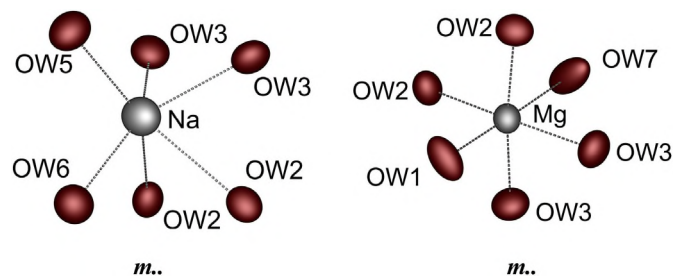
Fig. 3. The coordination environments of sodium (left) and magnesium (right) in NaMg[PO₃S]·9H₂O at room temperature, ellipsoids drawn on a 75% probability level, the site symmetries of Na and Mg are given.

Table 1
Data on the hydrogen bonds in NaMg[PO$_3$S]·9H$_2$O at room temperature; D = donor, A = acceptor; all values rounded to full pm and degrees.
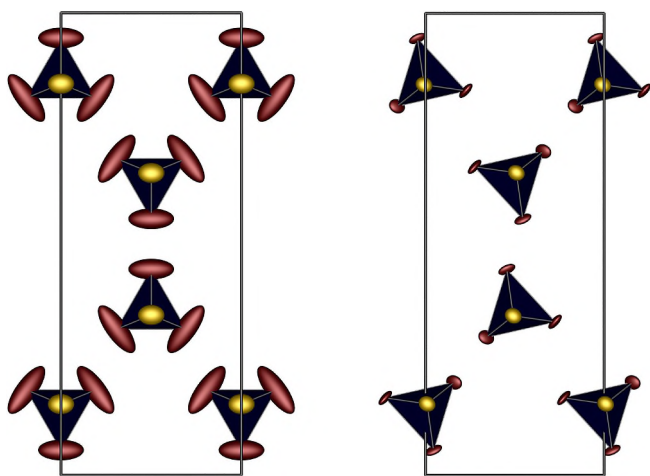
D–H	A	d(DH)/pm	d(HA)/pm	∡(DHA)/°	d(DA)/pm
OW1–H11	OW2	99(1)	184	175	283
OW1–H12	O2	98(1)	222	146	309
OW2–H21	S	98(1)	248	151	337
OW3–H31	O1	98(1)	170	167	267
OW3–H32	S	99(1)	225	172	323
OW4–H41	S	97(1)	228	172	325
OW4–H42	O2	98(1)	169	179	267
OW5–H51	O2	98(1)	166	173	263
OW6–H61	O2	99(1)	212	150	301
OW6–H61	O1	99(1)	259	131	332
OW7–H71	OW1	98(1)	174	167	271
OW7–H72	O1	99(1)	176	164	272

Table 2
Cell parameters of NaMg[PO$_3$S]·9H$_2$O at r. t. and at 100 K; given is also the twin matrix of the low-temperature structure refinement.

cell prmtr.	Cmc2$_1$ at 298 K	C112$_1$ at 100 K	twin matrix		
a/pm	638.58(4)	631.41(3)	−1	0	0
b/pm	1632.31(10)	1630.00(7)	0	1	0
c/pm	1217.16(7)	1219.24(5)	0	0	1
γ/°	90	90.00(2)			
V/10^6 pm	1268.72(13)	1254.84(10)			

$P2_1$ (no. 4) in a conventional setting. Both lost symmetry elements are preserved within the crystal leading to the twin law given in Table 2. Finally, we refined an ordered structure model of two twin domains with an approximate ratio 54.0(4):46.0(4). Since the structure relationships between high- and low-temperature form of NaMg[PO$_3$S]·9H$_2$O is easier to recognise we will describe the differences between both using the space group settings $Cmc2_1$ (HT-NaMg[PO$_3$S]·9H$_2$O) and $C112_1$ (LT-NaMg[PO$_3$S]·9H$_2$O). According to a group-subgroup scheme in the Bärnighausen formalism [16–19] the symmetry reduction is translationengleich of index 2 ($t2$). The essential change occurring upon phase transition is that the site of O2 within the PO$_3$S tetrahedron splits into O2A and O2B (Fig. 2). Thus an ordered arrangement of the PO$_3$S tetrahedra is achieved which can be nicely seen in Fig. 4. The bond-lengths and bonding angles remain in the same ranges (Table 3). The symmetry reduction by loss of a mirror plane from $Cmc2_1$ to

Table 3
Selected interatomic distances and angles for NaMg[PO$_3$S]·9H$_2$O at 298 K and at 100 K.

	298 K	100 K
interatomic distances/pm		
Na–O	231.0(4)–269.7(3)	230.2(5)–272.5(8)
Mg–O	202.2(3)–208.9(2)	201.7(5)–209.3(8)
P–O	150.1(3), 151.1(3)	153.2(6)–154.3(5)
P–S	204.7(1)	204.9(2)
angles/°		
O–P–O	109.2(2), 109.2(3)	109.0(3)–109.8(3)
O–P–S	109.2(1), 110.0(1)	108.6(2)–110.2(3)

$C112_1$ (translationengleicher $t2$ transition) causes a twinning of the observed crystals which has to be taken into account during the refinement.
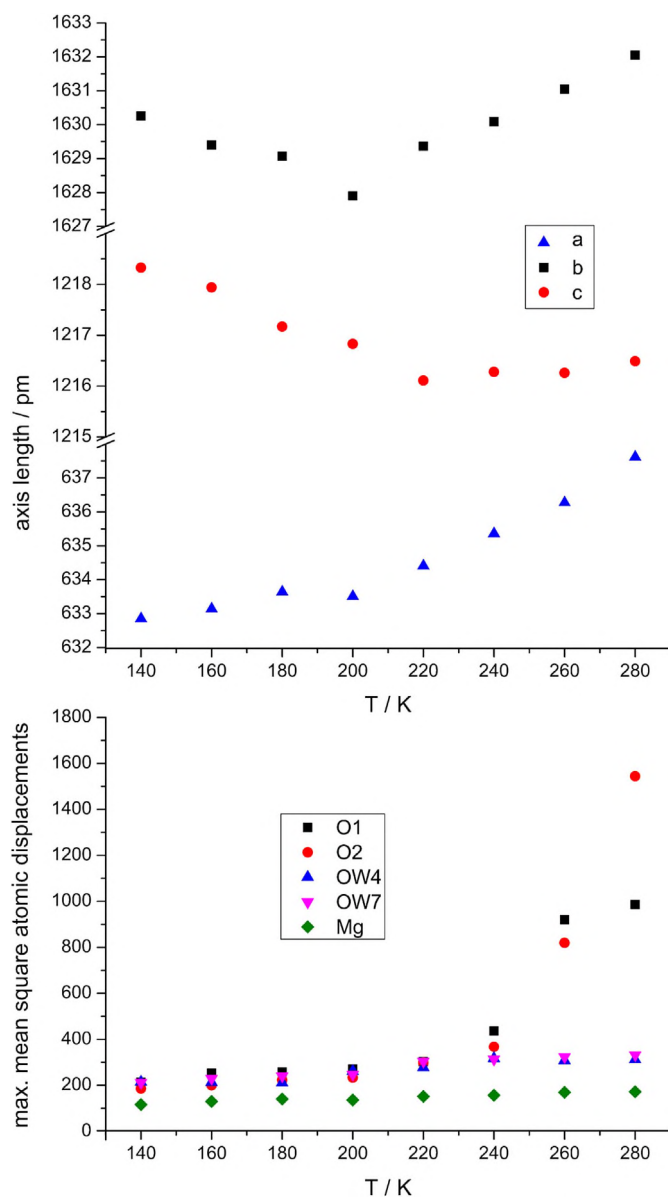
This order-disorder phase transition occurs between 200 and 240 K according to temperature-dependent single-crystal X-ray diffraction experiments between 140 and 280 K in steps of 20 K. At each step the lattice parameters were determined and a complete structure refinement was performed. Around 200 K the lattice parameters b and c pass through a minimum with a not significantly affected, and the mean square thermal displacement parameters of the atoms affected by the phase-transition grow significantly stronger than the unaffected ones (Fig. 5, top). Starting from high temperatures the increasingly inhibited mobility of the strongly vibrating PO$_3$S tetrahedra is in accordance with a slight increase of the lattice parameters b and c, a decreases further almost unaffected. This increase starts to happen below 220 K. Simultaneously, the mean square displacement parameters of the strongly vibrating atoms decrease significantly at the ordered sites of the two twin domains (Fig. 5, bottom) already below 240 K indicating the freezing process.

2.4. Vibrational spectra

The O–H bond of the crystal water molecules show stretching vibrations ν(OH) around 3089 cm^{-1} and a bending mode δ(OH) around 1615 cm^{-1}. The symmetric and asymmetric PO$_3$ -stretching modes νs(PO$_3$) and ν_{as}(PO$_3$) at 954 and 1032 cm^{-1}, respectively, are perceptible. The symmetric bending mode δ_s(PO$_3$) at 532 cm^{-1} and the asymmetric bending mode δ_{as}(PO$_3$) at 624 cm^{-1} can be observed, as well as the P–S stretching vibration ν_s(PS) at 459 cm^{-1} and the OPS bending mode δ_s(OPS) at 400 cm^{-1} (see also Fig. 6). The Raman Spectrum shows also the vibration of the O–H Bond ν(OH) around 3191 cm^{-1}, the asymmetric (ν_{as}(PO$_3$)) and the symmetric (ν_s(PO$_3$)) stretching vibration at 1061 cm^{-1} and 981 cm^{-1} of the PO$_3$ unit, as well as the asymmetric bending mode (δ_{as}(PO$_3$)) at 674 cm^{-1}. The P–S stretching vibration ν(PS) was observed at 456 cm^{-1}. These data are thus in accordance with our structure model.

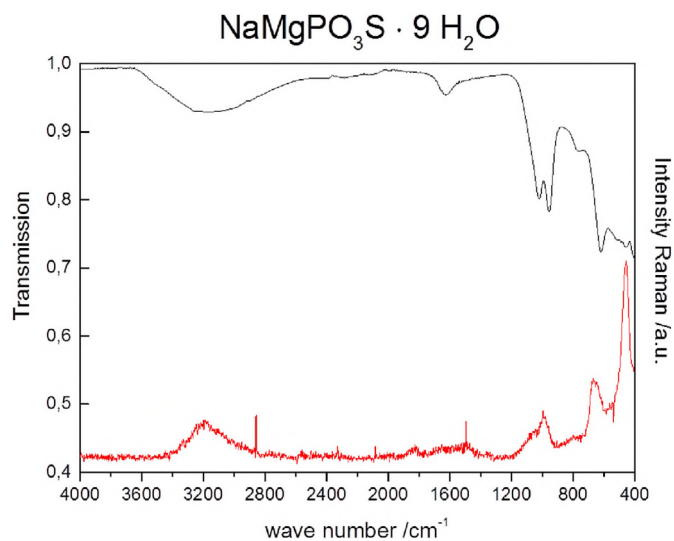### 2.5. ^{31}P solid state NMR spectroscopy

In Fig. 7 the solid state NMR spectrum of NaMg[PO$_3$S]·9H$_2$O is shown. The chemical shift of 33.7 ppm, recorded with respect to H$_3$PO$_4$ as reference, is in accordance with a monothiophosphate anion. The chemical shifts of the homologous calcium and barium compounds were determined to be 49 ppm for NaCa[PO$_3$S]·9H$_2$O and 34 ppm for NaBa[PO$_3$S]·9H$_2$O [12]. The tiny peak around 3.5 ppm is due to traces of a decomposition product containing orthophosphate formed during the measurement since the title compound is sensitive to temperatures above approx. 310 K.

Fig. 4. Dynamic and ordered arrangement of the monothiophosphate tetrahedra in NaMg[PO$_3$S]·9H$_2$O at r. t. (left) and at 100 K (right), oxygen atoms are drawn black, sulphur grey, ellipsoids drawn on a 90% probability level, both viewed along [001].
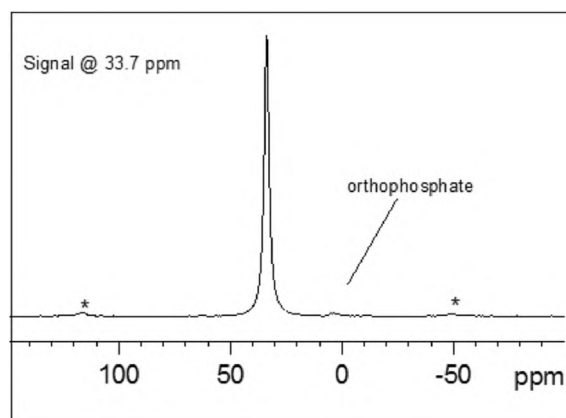
Fig. 5. Temperature-dependent development of the lattice parameters of NaMg[PO$_3$S]·9H$_2$O (top) and the maximal mean square atomic displacement parameters of selected atoms (bottom) given in $10^4 Å^2$ (Mg and the selected crystal water molecules remain almost unaffected by the phase transition and reflect the thermally induced behaviour); the error bars are smaller than the symbols of the data points.

Fig. 6. Vibrational spectra (top: IR; bottom: Raman) of NaMg[PO$_3$S]·9H$_2$O; the sharp Raman emission peaks at 1495 cm^{-1} and 2858 cm^{-1} are artefacts.

Fig. 7. Room temperature MAS-NMR-spectrum of NaMg[PO$_3$S]·9H$_2$O. The marked peaks represent rotational side bands.

of the PO$_3$S tetrahedra. This observed disorder might be expected since the monothiophosphate tetrahedra are coordinated solely by crystal water molecules without direct interaction with the sodium and magnesium ions. The phase transition is believed to be a topotactic order-disorder transition which could be followed by temperature-dependent single-crystal X-ray diffraction.

3. Experimental section

3.1. Syntheses

Trisodium monothiophosphate Na$_3$PO$_3$S was synthesized according to *Yasuda* [20]: 3.5 ml PSCl$_3$ (0.034 mol, Aldrich 98%) were added to a solution of 8 g NaOH in 60 ml demineralised water at 85°C. The product was subsequently precipitated by carefully dropping the clear aqueous solution in anhydrous methanol. The purity was checked by powder XRD and matched the literature data [5].

NaMg[PO$_3$S]·9H$_2$O: For the metathesis towards NaMg[PO$_3$S]·9H$_2$O, 2.78 mmol (500 mg, 2.78 mmol) Na$_3$PO$_3$S were dissolved in 16 ml demineralised water and added to a solution of MgCl$_2$·6H$_2$O (565 mg, 2.78 mmol) in 8 ml water. Complete precipitation was

2.6. Conclusions

In this contribution we shed light on the crystal structure of NaMg[PO$_3$S]·9H$_2$O which we obtained as a phase pure crystalline powder. In contrast to the homologous monothiophosphates NaCa[PO$_3$S]·9H$_2$O, NaBa[PO$_3$S]·9H$_2$O [12] and NaSr[PO$_3$S]·9H$_2$O [13] the magnesium compound adopts a polar orthorhombic structure at room temperature and represents a new structure type. Crystal structure determination, NMR spectrum as well as the vibrational spectra confirm unequivocally the presence of PO$_3$S moieties. Relatively large values of selected anharmonic displacement factors in the crystal structure pointed towards a possible symmetry reduction at low temperature. Indeed, below 240 K a symmetry reduction occurs from *Cmc*2$_1$ to *C*112$_1$ (conventional setting: *P*2$_1$) accompanied by a twinning comprising two different orientations

achieved by cooling the reaction mixture to $-5\,^{\circ}$C. After filtration and careful drying under vacuum $NaMg[PO_3S]\cdot 9H_2O$ was obtained as a colourless crystalline powder (yield: 92.2%).

3.2. Powder X-Ray diffraction

X-ray powder diffraction data of the title compound were collected at room temperature on a Bruker D8 Advance diffractometer equipped with a LynxEye 1-D detector (steps of 0.2°, acquisition time: 900 s/step, Soller slits 4°, fixed divergence slit 1 mm, transmission geometry) using Mo-K_{α} radiation at room temperature. The generator was set at 50 kV, 40 mA. The observed intensities are in very good agreement with the calculated diffraction pattern based on the single-crystal data (Fig. 8).

3.3. Single-crystal structure analyses of $NaMg[PO_3S]\cdot 9H_2O$

X-ray diffraction data were collected on a Bruker D8 Venture single-crystal diffractometer using Mo-K_{α} radiation at room temperature as well at 100 K. The crystal structure of $NaMg[PO_3S]\cdot 9H_2O$ at room temperature was solved by direct methods and refined using SHELXTL program package [21] in space group $Cmc2_1$ (no. 36) and with anisotropic displacement parameters for all atoms except the hydrogen ones. For the low temperature measurement at 100 K of $NaMg[PO_3S]\cdot 9H_2O$ holds basically the same procedure, but in this case the data were not averaged according to the orthorhombic unit cell; the structure refinement was performed in the non-conventional space group $C112_1$, i. e. $P112_1$ to be able to treat the twinning using an HKLF 4 file and a relatively simple twinning law; anisotropic displacement parameters for all atoms except the hydrogen ones were also refined. In both refinements the hydrogen atoms were located by difference Fourier syntheses and refined isotropically with fixed $U_{iso} = 0.04$ and commonly refined O—H distances of 97(1) pm. The relevant crystallographic data and further details of the X-ray data collection are summarised in Table 4. In Table 3 selected interatomic distances and angles are listed.

Further details of the crystal structure investigation presented in this work may be obtained from the Fachinformationszentrum Karlsruhe, D-76344 Eggenstein-Leopoldshafen, Germany (e-mail:

Table 4
Crystal structure data for $NaMg[PO_3S]\cdot 9H_2O$ at room temperature and at 100 K.

$NaMg[PO_3S]\cdot 9H_2O$	298 K	100 K
Data Collection		
ρ/g$\cdot$ cm^{-3}	1.678	1.696
R_{int}, R_σ	0.032, 0.034	0.115, 0.064
μ/mm^{-1}	0.51	0.52
block shape/colour	block/colourless	
crystal size	$0.05\times 0.03\times 0.02$ mm^3	
measured reflections	4273	10322
independent reflections	1225	1641
observed refl. ($F_o^2 \geq 2\sigma(F_o^2)$)	1116	1466
hkl range	$-7\leq h\leq 7$	$-6\leq h\leq 6$
	$-19\leq k\leq 19$	$-17\leq k\leq 17$
	$-14\leq l\leq 14$	$-13\leq l\leq 13$
theta range	$2\Theta<50.0^{\circ}$	$2\Theta<45.0^{\circ}$
Refinement		
BASF (twin)		0.460(4)
GooF	1.090	1.018
Flack parameter	0.12(12)	$-0.04(13)$
R1 (all)	0.036	0.045
wR2 (all)	0.071	0.070
residual max/min e$^-$ density	0.30, -0.20	0.21, -0.21

crysdata@fiz-karlsruhe.de) on quoting the depository numbers CSD-430072 ($NaMg[PO_3S]\cdot 9H_2O$, 298 K, $Cmc2_1$), CSD-430073 ($NaMg[PO_3S]\cdot 9H_2O$, 100 K, $C112_1$) and CSD-430074 ($NaMg[PO_3S]\cdot 9H_2O$, 100 K, $P112_1$) as well as the temperature-dependent structure refinements at 140 K (CSD-432028, $C112_1$), 160 K (CSD-432029, $C112_1$), 180 K (CSD-432030, $C112_1$), 200 K (CSD-432031, $C112_1$), 220 K (CSD-432032, $C112_1$), 240 K (CSD-432033, $C112_1$), 260 K (CSD-432034, $Cmc2_1$), 280 K (CSD-432035, $Cmc2_1$), the names of the authors, and citation of this publication.

3.4. Vibrational spectroscopy

The Infrared Spectrum was recorded with a Bruker Equinox 55 FT-IR with platinum ATR unit and analysed with RefFIT [22]. The Pellet of 2 mg sample and 300 mg KBr was measured with a Bruker FRA 106/S Module, with a YAG:Nd Laser ($\lambda = 1064$ nm). The scanning range for both was from 400 to 4000 cm^{-1}. The Raman spectrum was measured on a Bruker FRA 106/S module ($\lambda = 1064$ nm) scanning a range from 400 to 4000 cm^{-1} (Universität Freiburg).

3.5. NMR spectroscopy

The MAS NMR spectrum was recorded with a Bruker AVANCE III by Prof. van Wüllen (Universität Augsburg).

Appendix A. Supplementary data

Supplementary data related to this article can be found at http://dx.doi.org/10.1016/j.solidstatesciences.2016.10.009.

References

[1] Henning A. Höppe, New developments of inorganic phosphors, Angew. Chem. Int. Ed. Engl. 48 (2009) 3572—3582.
[2] F.C. Mijlhoff, J. Portheine, C. Romers, The crystal structure of tetragonal p4o6s4, Recueil des Travaux Chimiques des Pays-Bas 86 (3) (1967) 257—262.
[3] F. Frick, M. Jansen, Crystal structure of 2,4,6,8,10-hexaoxa-1,3,5,7-tetraphosphatricyclo [3.3.1.1] decane 1,3,5,7-tetrasulfide, o6p4s4, Z. Kristallogr. Cryst. Mat. 209 (12) (January 1994) 985.
[4] B.M. Goldstein, Disorder in the structure of trisodium phosphorothioate dodecahydrate na3po3s.12h2o, Acta Crystallogr. B 38 (1982) 1116—1120.
[5] M. Pompetzki, M. Jansen, Natriummonothiophosphat(v): kristallstruktur und natriumionenleitfähigkeit, Z. Anorg. Allg. Chem. 628 (3) (2002) 641—646.
[6] M. Pompetzki, L. van Wüllen, M. Jansen, Festkörper-nmr-untersuchungen an
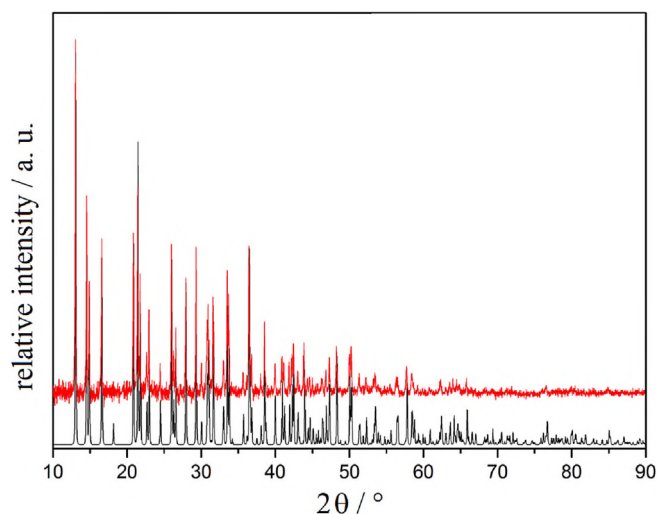
Fig. 8. X-ray powder diffraction patterns of $NaMg[PO_3S]\cdot 9H_2O$ (red) and calculated X-ray powder diffraction pattern from single-crystal data of $NaMg[PO_3S]\cdot 9H_2O$ (black). (For interpretation of the references to colour in this figure legend, the reader is referred to the web version of this article.)

natriumoxothiophosphaten(v), Z. Anorg. Allg. Chem. 630 (3) (2004) 384−388.

[7] Vitalijus Janickis and Kjartan. Maroey. The dihydrogen monothiophosphate and trihydrogen disulfanediphosphonate anions. crystal structures of kh2spo3 and [co(en)2cl2]h3s2p2o6, Acta Chem. Scand. 48 (6) (1994) 461−464.

[8] J. Neels, K.-H. Jost, M. Meisel, K.K. Palkina, S.I. Maksimova, N.T. Tshibiskova, Darstellung und kristallstrukturuntersuchungen einiger biureto(thio)phosphate, Z. Anorg. Allg. Chem. 540 (9−10) (1986) 307−318.

[9] M. Meisel, G.U. Wolf, M.T. Averbuch-Pouchot, Structure of guanidinium 1,2,3,4-tetrathio-cyclo-tetraphosphate, Acta Crystallogr. C 46 (11) (Nov 1990) 2239−2241.

[10] Alexander E. Gash, Peter K. Dorhout, Steven H. Strauss, Zirconium and hafnium hydrogen monothiophosphates, h2zr(po3s)2 and h2hf(po3s)2. syntheses and selective ion-exchange properties of sulfur-containing analogues of h2m(po4)2 (m = zr, hf), Inorg. Chem. 39 (24) (2000) 5538−5546.

[11] Nathan J. Takas, Jennifer A. Aitken, Phase transitions and second-harmonic generation in sodium monothiophosphate, Inorg. Chem. 45 (7) (2006) 2779−2781.

[12] Karolina Kazmierczak, Joachim G. Heck, Henning A. Höppe, Syntheses, crystal structures, vibrational spectra and 31p mas nmr spectra of the thiophosphates nam(po3s)9h2o (m = ca, ba), Z. Anorg. Allg. Chem. 636 (2010) 409−413.

[13] Mimoza Gjikaj, Crystal structure of sodium strontium monothiophosphate nonahydrate, nasr[po3s]9h2o, Z. Kristallogr. NCS 223 (2008) 1−2.

[14] R.D. Shannon, Revised effective ionic radii and systematic studies of interatomie distances in halides and chalcogenides, Acta Crystallogr. A 32 (1976) 751−767.

[15] Thomas Steiner, The whole palette of hydrogen bonds, Angew. Chem. Int. Ed. Engl. 41 (2002) 48−76.

[16] Hartmut Bärnighausen, Group-subgroup relations between space groups: a useful tool in chrystal chemistry, Commun. Math. Chem. 9 (1980) 139−175.

[17] Ulrich Müller, Symmetry relations between space groups, in: second ed., in: H. Wondratschek, Ulrich Müller (Eds.), International Tables for Crystallography, vol. A1, John Wiley & Sons Ltd., Chichester, 2010, pp. 428−722.

[18] Ulrich Müller, Kristallographische gruppe-untergruppe-beziehungen und ihre anwendung in der kristallchemie, Z. Anorg. Allg. Chem. 630 (11) (2004) 1519−1537.

[19] U. Müller, Symmetriebeziehungen zwischen verwandten Kristallstrukturen: anwendungen der kristallographischen Gruppentheorie in der Kristallchemie, Studienbücher Chemie. Vieweg+Teubner Verlag (2012).

[20] Stanley K. Yasuda, Jack L. Lambert, Sodium monothiophosphate, Inorg. Synth. 5 (1957) 102−104.

[21] Madison Siemens Analytical Xay Instruments Inc, Shelxtl x-ray single crystal analysis system, version 5.1, SHELXTL X-Ray Single Crystal Analysis System, Version 5.1 1 (1997) 1−154.

[22] A. Kuzmenko, Guide to RefFIT Software to Fit Optical Spectra, 2010.